

Material Characterization and Electrical Performance of *Prosopis Africana* Conductive Ink for Antenna Applications

Suleiman Babani^{1,3}, Mohd Nizar Hamidon^{1*}, Alyani Ismail², Haslina Jaafar²,
Intan Helina Hasan¹, Farah Nabilah Shafiee¹, Ibrahim Garba Shitu¹,
Jamila Lamido³, Sani Halliru Lawan³ and Zainab Yunusa⁴

¹Institute of Nanoscience & Nanotechnology (ION2), Universiti Putra Malaysia, 43400 UPM Serdang, Selangor, Malaysia

²Faculty of Engineering, Universiti Putra Malaysia, 43400 UPM Serdang, Selangor, Malaysia

³Department of Electrical Engineering, Faculty of Engineering, Bayero University Kano, PMB 3011 Kano, Nigeria

⁴Department of Electrical Engineering, University of Hafr Al Batin City, 39524, Saudi Arabia

ABSTRACT

This research explores the development and evaluation of a bio-based conductive ink derived from *Prosopis Africana* Char (PAC) for antenna applications, aiming to provide a sustainable, cost-effective alternative to conventional conductive materials in electronics. The study focuses on the structural, thermal, and electrical properties of the PAC-based ink to determine its suitability for printed antenna technology. The conductive ink was formulated by mixing PAC powder with an organic binder composed of m-xylene, linseed oil, and α -terpineol in a 45:55 wt% ratio, followed by mechanical stirring at 250 rpm for 3 hours at 40 °C to achieve a homogeneous paste. This mixture

was screen-printed onto an FR4 substrate and thermally treated at 300 °C. Characterization techniques such as field emission scanning electron microscopy (FESEM), Raman spectroscopy, thermogravimetric analysis (TGA), and four-point probe conductivity measurements were used to analyze the ink's morphology, composition, and electrical behavior. The PAC ink demonstrated a high conductivity of 4.678 S/m, strong adhesion, and excellent printability and environmental stability under variable temperature and humidity. Antenna performance assessments revealed promising results, including a return loss of $|S_{11}| = -16.50$ dB, a resonant frequency of 9.5

ARTICLE INFO

Article history:

Received: 01 April 2024

Accepted: 10 April 2025

Published: 10 June 2025

DOI: <https://doi.org/10.47836/pjst.33.S4.02>

E-mail address:

sbabani.ele@buk.edu.ng (Suleiman Babani)

mnh@upm.edu.my (Mohd Nizar Hamidon)

alyani@upm.edu.my (Alyani Ismail)

jhaslina@upm.edu.my (Haslina Jaafar)

i_helina@upm.edu.my (Intan Helina Hassan)

farahnabilahshafiee@gmail.com (Farah Nabilah Shafiee)

ibrahimgarbashitu@gmail.com (Ibrahim Garba Shitu)

sumailajamila@gmail.com (Jamila Lamido)

shlawan.ele@buk.edu.ng (Sani Halliru Lawan)

zainaby@uhb.edu.sa (Zainab Yunusa)

*Corresponding author

GHz, a bandwidth of 1.32 GHz, a peak gain of 6.62 dB, a VSWR of 1.25, and an efficiency of 80%. These outcomes indicate that the PAC thick film enhances bandwidth and radiation efficiency due to its favorable dielectric characteristics. Overall, the study confirms the potential of *Prosopis africana* as a viable, eco-friendly conductive material for flexible, lightweight antennas, offering a promising direction for sustainable innovation in wireless communication technologies.

Keywords: Bandwidth, electrical conductivity, material analysis, micrometersized PAC powder, *Prosopis africana* conductive ink, sustainable patch antenna fabrication, thick film

INTRODUCTION

The conventional microstrip patch antenna (MPA) design consists of three main components: a radiating patch, a substrate, and a ground plane. Unlike traditional microwave antennas, microstrip patch antennas offer several advantages, such as being lightweight, flat profile, cost-effective, and easy to fabricate. However, choosing an MPA over traditional antennas requires careful consideration of some limitations, including low efficiency and narrow bandwidth (Bansal, 2008). Therefore, selecting the right substrate material is crucial in achieving optimal performance tailored to the specific requirements or application of the device. Microstrip antennas were first developed in the 1950s, and since then, there have been significant advancements in printed circuit board (PCB) technology, particularly in the 1970s. These antennas come in different shapes and sizes, but rectangular and circular patches are the most common due to their ease of design and suitability for array configurations (Garg et al., 2001). Patch antennas have traditionally been made using copper as the primary radiating material (Babani et al., 2015). However, producing copper can cause environmental pollution, and the oxidation that occurs after fabrication can lead to a decrease in the performance of the antenna (Ram et al., 2021). Therefore, finding an alternative material to replace copper in printed electronics remains a significant challenge.

Previous research has extensively examined the use of carbon-based materials, such as carbon nanotubes, graphene, carbon black, and graphite, as conductive patch elements. Some of the work has become increasingly interested in carbon-based material printed antennas (Lu et al., 2021; Quaranta et al., 2019), sensors (Bakar et al., 2023; Guo et al., 2021), energy storage and conversion (Husain et al., 2022) and electromagnetic devices (Alshahrani & Prakash, 2023; Huo et al., 2023), due to their excellent properties, such as electrical, mechanical, and chemical stability, cost-effectiveness, and lightweight characteristics (Khair et al., 2019; Lu et al., 2022).

In the study conducted by Ram et al. (2021) on graphene circular structures, a circular microstrip patch array (MPA) based on graphene was employed, resulting in an enhancement of gain by approximately 5 dBi. Another investigation has been documented, incorporating graphene properties into CST and COMSOL simulations (Su et al., 2016).

Song et al. (2019) conducted a separate research endeavor wherein a 2×2 rectangular patch array was fabricated through the laser engraving of a graphene film, followed by its transfer onto a substrate. This process is acknowledged for its complexity and high cost. Devi et al. (2017) introduced a novel rectangular microstrip antenna employing carbon nanotubes (CNTs) to achieve a broad bandwidth, and the antenna demonstrated a notable improvement with a 20% increase in impedance bandwidth.

Additionally, employing graphene-based materials as conductive patches, as highlighted by Azman et al. (2022), results in a notable 60% increase in bandwidth. In the field of communication systems, there is a crucial need to improve bandwidth for practical use. The challenges in designing radio frequency (RF) antennas that use nanomaterials are related to identifying the resonance of materials at lower or higher frequencies and establishing reliable electrical connections with nanomaterials to assess performance.

One of the most promising approaches is using natural materials, which provide sustainability and improve performance. In this regard, *Prosopis Africana*, a sustainable natural resource, has gained considerable interest due to its unique electrical characteristics and the practicality of producing conductive ink from its biomass (Babani et al., 2023).

However, a new proposal has emerged to investigate the conversion of *Prosopis africana* biomass into a similar carbon-based material. This idea is based on recognizing *Prosopis africana* as a versatile tree with significant economic importance in rural and urban communities across sub-Saharan Africa (Agboola, 2004; Nnamani et al., 2020).

The primary objective of this study is to present a novel approach to antenna design by harnessing the properties of *Prosopis africana* as a replacement for copper due to its higher conductivity, to develop a conductive ink-based patch antenna. The central focus of this research is on enhancing the bandwidth of patch antennas, a crucial parameter for modern communication systems, including Wi-Fi, 5G, and satellite communication.

Prosopis africana biomass, derived from the tree species native to sub-Saharan Africa, is recognized as a valuable and multifaceted natural resource. This biomass is extensively utilized across various domains, encompassing traditional roles in food production, medicinal practices, and timber supply, as well as modern applications in sustainable energy, environmental protection, and the development of advanced materials (Bishop et al., 2021). Additionally, the tree's pods serve as a source of nutrient-rich fodder and possess medicinal properties, underscoring their importance for livestock and human sustenance, particularly in arid environments (Yusuf et al., 2008).

Prosopis africana biomass is increasingly utilized for bioenergy production, serving as a renewable and environmentally friendly source of fuel and electricity (Kiflie et al., 2023). Additionally, its capacity to thrive in diverse climatic conditions and its potential to rehabilitate degraded landscapes underscore its importance in mitigating desertification and promoting land restoration. Pyrolysis, as the preliminary step in the thermochemical

conversion of biomass, involves complex mechanisms influenced by various factors, including the material's composition, particle size, heating rate, and other related parameters (Rao & Sharma, 1998).

Biochar, a carbon-rich substance generated through biomass pyrolysis, has gained attention as a promising material for diverse electronic applications (Yan et al., 2022). Its distinct characteristics, including high carbon content and excellent electrical conductivity, render it an appealing option for various electronic components. The material's significant surface area and porosity facilitate efficient charge storage, thereby enhancing its energy storage capacity (Leng et al., 2021). Moreover, the abundant carbon structure of biochar can be tailored or functionalized to enhance its electrochemical performance, positioning it as a versatile and sustainable solution for developing cost-effective energy storage technologies.

The compatibility of biochar with flexible electronics warrants particular attention. Its unique mechanical flexibility and electrical conductivity combination positions biochar as a promising candidate for use in flexible and wearable electronic devices (Rizwan et al., 2017). Incorporating biochar into electronic applications signifies progress toward developing sustainable and eco-friendly technological innovations (Tovar-Lopez, 2023).

Thick film processing is a popular method for electronic applications due to its simplicity, speed, and cost-effectiveness. This technique allows for incremental layer deposition, which can be tailored to the specific requirements of the application. It also contributes to the miniaturization of electronic devices (Shafee et al., 2020).

This study introduces a new approach to developing a thick film paste for PAC, which combines micro-sized powder and an organic binder. This unique paste formulation is an important contribution not previously documented. By using thick film technology, we are now able to create an MPA with improved performance utilizing the commonly used FR4 substrate.

METHOD AND MATERIAL

The study used raw material from *Prosopis africana*, a widespread plant species in northern Nigeria. The materials were collected from Duhun Karo farms in the Hadejia Local Government Area of Jigawa State, Nigeria. The *Prosopis africana* wood was subjected to controlled pyrolysis to obtain activated char. The carbonization process was carried out at optimized temperatures and durations, resulting in PAC with desired properties at 500 °C for 3 hours. Figure 1 shows a step-by-step process for synthesizing PAC through pyrolysis (Kiflie et al., 2023). The carbonized material was then crushed into powder using a mortar and pestle. After that, the PAC powder was sieved to a micrometer size of <20 microns, which served as the active material in fabricating thick film antennas (Figure 2).

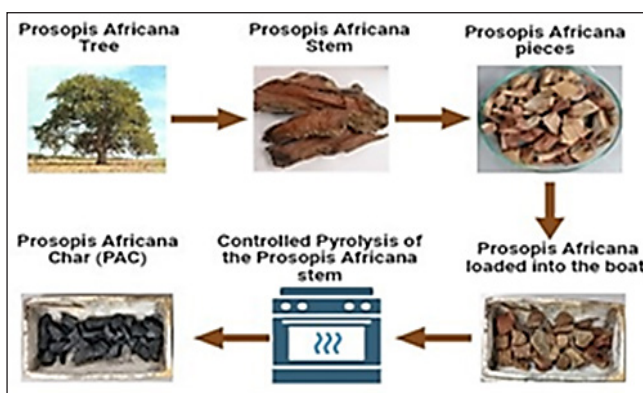


Figure 1. Preparation of activated char from *Prosopis africana* biomass (Babani et al., 2024a)



Figure 2. (a) The process of crushing PAC material using a mortar and pestle after carbonization, and (b) the process of sieving the PAC Powder using a < 20 micron sieve

The paste formulation commenced by blending PAC micrometer powder of 45 wt% with an organic binder of 55 wt%, comprising (M-X), (LO), and (α -T). The chemical composition remained unchanged post-purchase. The selection of the active powder ratio was informed by prior research (Hasan et al., 2018). The amalgamation was stirred at 250 rpm for 3 hours, maintaining a temperature of 40 °C using a magnetic stirrer to achieve a homogeneous consistency. Figure 3 illustrates the process formulation of organic volatiles (OV) and PAC powder employed for the thick film paste.

After mixing, the paste was applied onto an FR4 substrate using a silk screen with a rectangular design. The PAC thick film was given 10–15 minutes to level off, dried, and then fired in a box furnace at 300 °C for 60 minutes. This process aimed to eliminate the organic binder and securely bind the nano-powders to the substrate (Shafiee et al., 2020). Various techniques were used to characterize the thick, dried PAC film. Raman

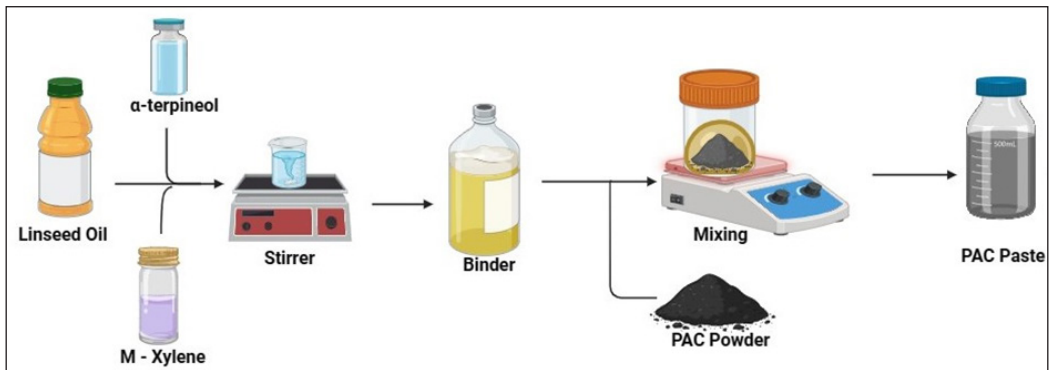


Figure 3. Formulation of organic binder and PAC paste thick film for screen printing

spectroscopy was used to assess the graphitic defects in the PAC powder, field emission scanning electron microscopy (FESEM) was used to analyze the structural morphology, and energy dispersive x-ray spectroscopy (EDX) was conducted for elemental analysis of the PAC thick film. A thermogravimetric analysis (TGA) was employed to determine the thermal stability of the PAC paste.

After characterization, a PAC thick film was printed onto a one-sided FR4 substrate, which served as both the antenna feedline and radiating patch. The antenna design was carefully simulated and optimized after inserting all the dimension values and associated PAC values as a new material into the CST software to determine the ideal and geometrical parameters, ensuring the desired bandwidth enhancement. After the design stage, the patch was printed and fired at 150 °C for 30 minutes. Then, an SMA connector was attached to the fabricated antenna to enable the measurement of resonant frequency, return loss, and bandwidth via the vector network analyzer (VNA). The structure of the antenna design and the physically fabricated MPA can be seen in Figure 4. This design was simulated to work at the resonant frequency of 9.50 GHz for airborne radar applications.

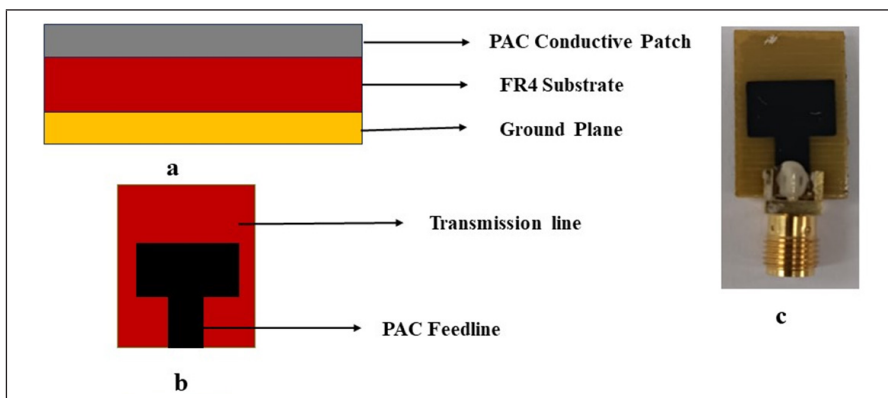


Figure 4. MPA structure: (a) view from the side, (b) view from the top, (c) fabrication prototype

RESULTS AND DISCUSSION

Graphitic materials are characterized by their black color and similar densities, which makes it crucial to distinguish between them accurately. Performing standard characterization procedures on sp² graphitic materials is customary before conducting any tests. Raman spectroscopy is the most effective method for such characterization (Kusaimi et al., 2018; Shitu et al., 2024). The results of Raman spectroscopy for the milled PAC powders are presented in Figure 5. In order to gain a better understanding of the graphitization process in activated charcoal, a Raman analysis was conducted. The graph shows two distinct peaks at 1358 cm⁻¹ and 1580 cm⁻¹, representing the defect mode (D band) and graphitic mode (G band). The calculated value of the ratio of defect intensity (I_D) to graphitic intensity (I_G), (I_D/I_G), is 0.98. This indicates a significant level of disorder associated with defects in the graphitic structure. These peaks are associated with graphene and graphite (Chen et al., 2016; Shitu et al., 2023).

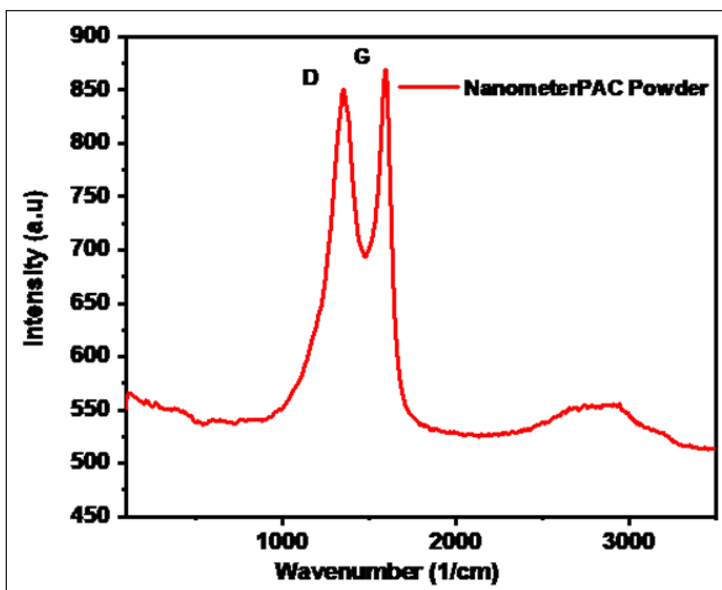


Figure 5. Raman of PAC powders

Figure 6 displays FESEM images illustrating the PAC thick film at room temperature and fired at 300 °C. Before being subjected to the specified temperature, the thick film was covered with a liquid organic binder (OB). Upon firing in the furnace, the binder underwent drying and evaporation, which encased the nanoparticles and bound them to the substrate. The OB, which contained linseed oil (LO), a drying oil, demonstrated polymerization upon exposure to the designated temperature. This property makes the oil suitable for a binder and a thick film paste. The FESEM image of the thick film fired at 300 °C shows a well-

dispersed arrangement of PAC powder, displaying nanoparticles within the range of 10 to 20 nm (Hasan & Hamidon, 2017; Yunusa & Musa, 2023).

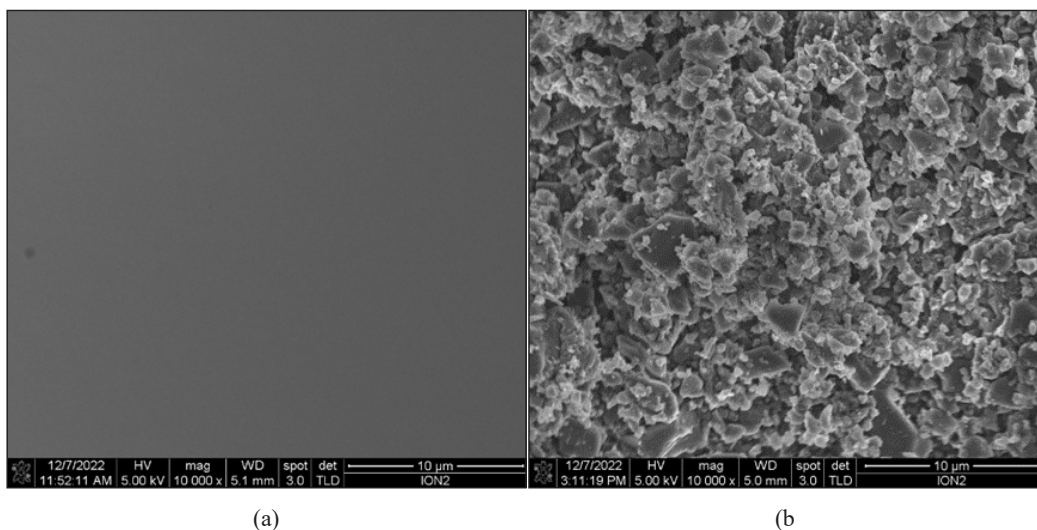


Figure 6. Morphology of PAC film (a) at room temperature and (b) firing at 300 °C

Figure 7 depicts the results of the EDX analysis conducted on both samples, which confirms the impact of firing temperature. The analysis revealed that the carbon component in the OV decreased while other elements associated with the PAC material increased as the firing temperature increased. These findings suggest that the elevated temperature facilitated the volatilization or desiccation of the OV, mainly composed of LO, exposing the nanoparticles underneath the oil layer (Babani et al., 2024b). To summarize, the analysis of samples processed at 300 °C showed conspicuous visibility of nanoparticles on the thick film's surface, which could affect the material's properties and overall performance (Abadi, 2010). After firing, the EDX analysis of the thick film surface indicates a higher carbon content in C: O elements, attributed to the presence of LO and other solvents at this stage.

Figure 8 shows the weight loss and decomposition rate of PAC paste in the temperature range of 25 to 1000 °C under an air atmosphere. The paste's volatile components evaporate between 50 °C and 255 °C, which corresponds to the flash point and boiling point of M-X (25 °C, 138 °C) and (α .T) (90 °C, 217 °C), respectively (Hasan et al., 2018). After that, non-volatile constituents, mainly LO, are removed. According to material specification documents, LO has a flash point of 300 °C and a boiling point of over 400 °C. The boiling of LO becomes prominent, with its boiling point reaching a maximum of 376 °C and beyond. In the final stages of this thermal process, a secondary decomposition event occurs within the temperature range of 400 °C to 500 °C, which is directly associated with the breakdown of linseed oil. Almost all the OV have evaporated and disintegrated by this point, leaving

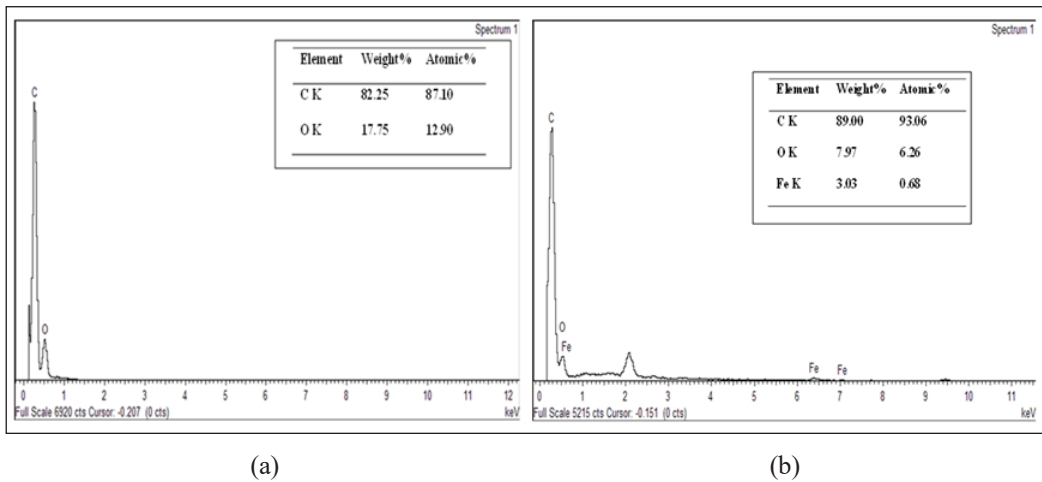


Figure 7. EDX of PAC film at (a) room temperature and (b) at firing temperature at 300 °C

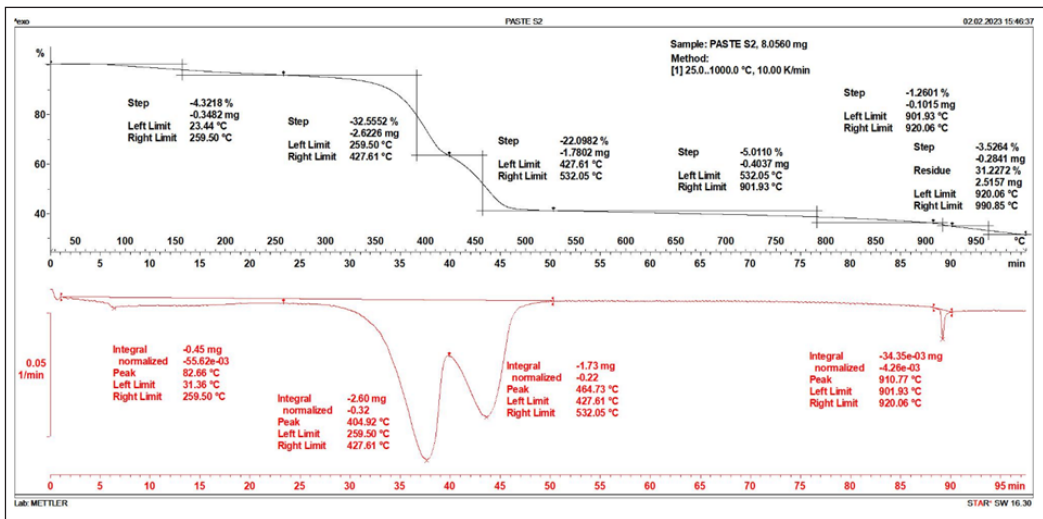


Figure 8. TGA measurement of PAC paste thick film

the PAC ashes firmly adhered to the alumina substrate. Therefore, it can be concluded that the optimal temperature range for PAC thick films, using LO as its OV, is between 400 °C and 500 °C. LO is a suitable organic vehicle within this range for formulating viscous films that can withstand lower firing temperatures (Sumaila et al., 2023a).

The electrical characterization was conducted using a four-point probe setup to determine the electrical resistance of the thick films. The relevant electrical parameters, such as sheet resistance, resistivity, and conductivity, were calculated using the appropriate formulas:

$$\text{From Ohm's law } R = \frac{V}{I} \quad [1]$$

$$R_S = R * R_{CF} \quad [2]$$

$$\rho = R_S * t \quad [3]$$

$$\delta = \frac{1}{\rho} \quad [4]$$

where R is the resistance in Ω , R_{CF} is the correctional factor that depends on the thickness of the film, ρ is the resistivity in Ω/m , t is the thickness of the PAC thick film in μm , and δ is the conductivity in S/m. From four points, the values of $R = 2.10E3$, $R_{CF} = 8.186$, $R_S = 1.7191E4$, and $t = 12.43 \mu m$ are the average thickness from the cross-sectional FESEM. Therefore, we calculated the resistivity and conductivity from the above formula as $\rho = 0.2137 \Omega/m$ and $\delta = 4.679$ S/m, respectively. From Table 1, it shows that the summary of the 45 wt% of PAC has good electrical conductivity, which is due to the amount of binder removed during the annealing process and the particle shape, size, and particle interconnection, similar to studies (Babani et al., 2025; Sumaila et al., 2023b).

Table 1
The electrical conductivity of the PAC thick film

| Material | Resistance (Ω) | Sheet Resistance (Ω/sqr) | Resistivity (Ω/m) | Conductivity (S/m) |
|----------|-------------------------|-----------------------------------|----------------------------|--------------------|
| PAC | 2.10E3 | 1.7191E4 | 0.2137 | 4.679 |

A preliminary simulation was conducted to prepare for the fabrication of the MPA component. The goal was to determine the design parameters and dimensions for both the substrate and the radiating patch. Even small changes to these dimensions can significantly affect the MPA's performance, making the simulation phase a crucial step in the fabrication process. In this study, the operational frequency for the MPA was set at 9.50 GHz, complying with ITU regulations for the X-band specifications. FR4 was selected as the substrate material, and PAC paste was used for the feedline and patch during the simulation to define the dimensions of both the substrate and the patch. The thickness and substrate height of the radiating patch, represented by 't' and 'h', respectively, are usually kept below the wavelength. The FR4 substrate is characterized by a relative permittivity of 4.3 and has a thickness of 1.6mm, a 0.035 mm copper thickness, and a conductive PAC thickness of 0.01923 mm.

Figure 9 also presents the analysis of MPA performance with PAC thick film on an FR4 substrate within a frequency range of 8 to 11 GHz. Both simulation and experimental measurements were conducted to assess the impact of the PAC thick film as a conductive radiating patch on the simulated resonant frequency of 9.5 GHz.

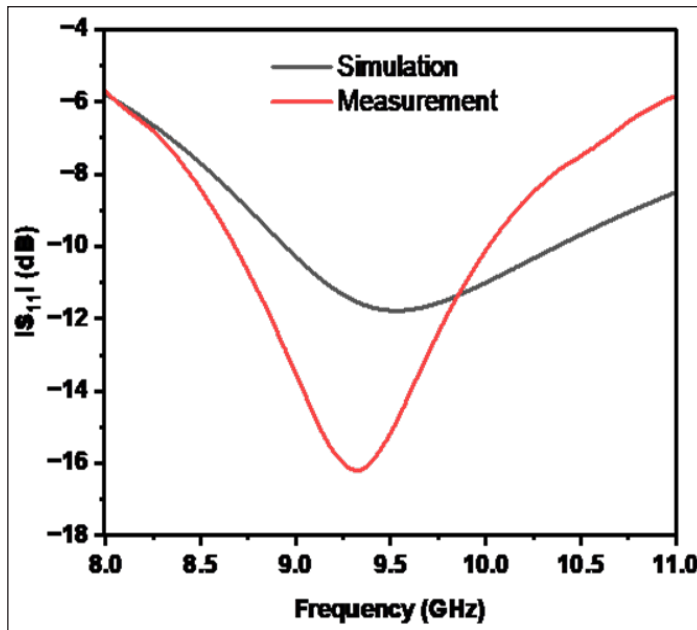


Figure 9. Return loss of the simulated and measured results of the PAC thick film MPA

A detailed comparison between simulation and measurement results is provided, and a summary of all data is tabulated in Table 2. These findings reveal that the MPA fabricated with the PAC thick film significantly enhances return loss, bandwidth, and gain.

Table 2
Summary of simulated and measurement values

| Parameters | Simulation Value | Measurement Value |
|-------------------------------------|------------------|-------------------|
| Operating Frequency (GHz) | 9.5 | 9.38 |
| Return loss S ₁₁ (dB) | -11.50 | -16.50 |
| Bandwidth @ -10dB (GHz) | 1.41 | 1.32 |

The graph showcases the 9.5 GHz frequency for $\Phi = 90^\circ$ and $\Phi = 0^\circ$, drawing attention to the variations and contrasts in radiation levels across the substrate. By providing a clear depiction of the frequency's behavior in a two-dimensional plane, it becomes easier to pinpoint areas of differing radiation intensities, as demonstrated in Figure 10. This type of analysis is vital for applications that depend on accurate frequency control and enhanced signal optimization (Musa et al., 2023).

A simulation was performed to analyze the peak realization gain on the substrate. The analysis at 9.5 GHz offers critical insights into the system's robustness and reliability. This frequency-specific information is essential for optimizing the system's performance

and ensuring its functionality under optimal conditions. Such detailed evaluation plays a pivotal role in developing and refining frequency-sensitive technologies, improving their effectiveness. Figure 11 presents the simulated peak realization gain, measured at 6.68 dB.

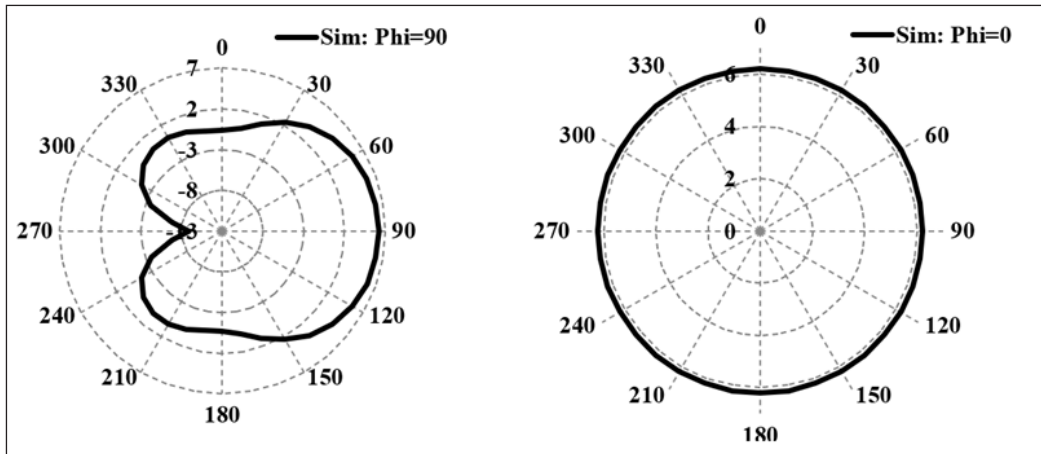


Figure 10. The simulated 2D radiation pattern of the proposed antenna

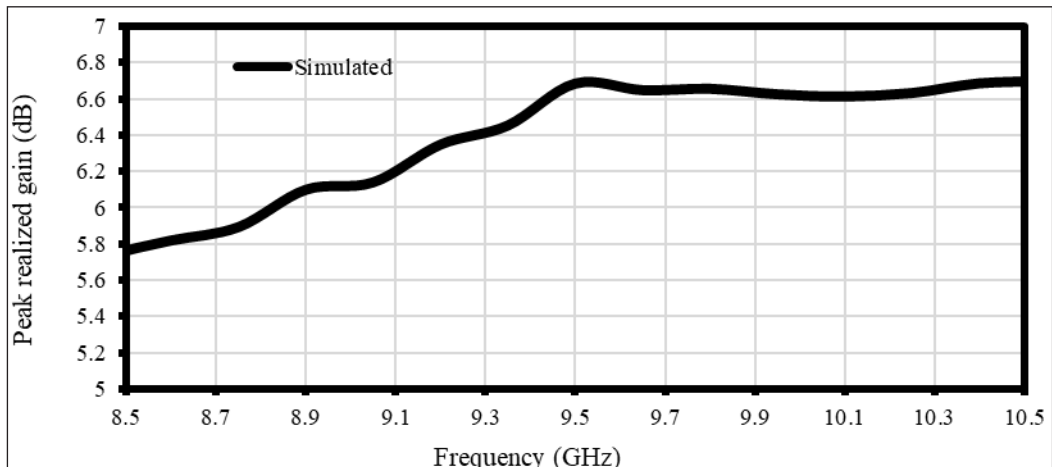


Figure 11. The simulated peak realized gain vs frequency on the substrate

As shown in Table 3, this research marks an important progression in enhancing the bandwidth of MPAs to meet the increasing requirements of modern communication and sensing systems. The effective implementation of PAC ink suggests novel opportunities for incorporating sustainable materials into radar technologies, fostering advancements in antenna design and materials science. The outcomes of this study motivate further investigation into achieving more sustainable and efficient wireless communication and radar systems (Babani et al., 2024a; Muhammad et al., 2021; Musa et al., 2023).

Table 3

Comparison study of patch antennas over different carbon materials on X Band

| Antenna | f_0 (GHz) | Conductive Patch Material | $ S_{11} $ (dB) | BW (GHz) | Gain (dB) | Application | Ref. |
|------------------|-------------|---------------------------|-----------------|-------------|-------------|-----------------------|------------------------------------|
| <i>R</i> | 10.00 | MWCNT | -15.50 | N.A | 1.20 | X- Band | (Dakshayani & Suryanarayana, 2022) |
| <i>R</i> | 10 | MWCNT | -11.64 | 2.5 | 0.81 | BW enhancement | (Devi et al., 2017) |
| <i>R</i> | 11.04 | Graphene | -12.05 | 1.45 | N.A | 5G | (Sa'don et al., 2019) |
| <i>R</i> | 11.0 | Graphene | -16.20 | 0.814 | 6.54 | Military satellites | (Yunusa & Shehu, 2022) |
| This Work | 9.5 | PAC | -16.50 | 1.32 | 6.68 | Airborne Radar | |

R = Rectangular Patch Antenna

CONCLUSION

Material characterization and performance analysis serve as essential tools for evaluating the suitability of materials in various applications. This study emphasized the relationship between intrinsic properties, processing methods, and performance outcomes, offering an in-depth understanding of the material behavior under specific conditions. The research outcomes underscore the importance of leveraging advanced characterization techniques to refine material properties and enhance functionality. This work bridges the gap between theoretical material science and practical engineering applications by correlating experimental data with application-specific requirements. Ultimately, this study contributes to the ongoing efforts to innovate in material selection and design, addressing current challenges and future opportunities. Continued exploration into emerging materials and cutting-edge analysis techniques will be critical in shaping the next generation of high-performance materials.

In conclusion, this article contributes to the growing body of knowledge on material characterization and performance by presenting a detailed and practical framework for evaluating materials for any electronics applications that require electrical conductivity, like antenna and sensor applications, because of the higher electrical conductivity of 4.46 S/m. The research underscores the necessity of linking characterization data to real-world performance to drive innovation in material design and development. Future work could explore [specific suggestions] to further refine the material's applicability across broader contexts and enhance its role in advancing technological solutions.

ACKNOWLEDGEMENTS

This work was supported by the Petroleum Technology Development Fund (PTDF) of Nigeria. The Faculty of Engineering's Putra-IPS Grant/2022/9735300 and the Institute of Nanotechnology and Nanoscience (ION2) at Universiti Putra Malaysia (UPM) also provided financial assistance.

REFERENCES

- Abadi, M. H. N. S. (2010). *Development of nanocrystalline thick film gas sensors* [Unpubliss doctoral thesis]. Universiti Putra Malaysia.
- Agboola, D. A. (2004). *Prosopis africana* (Mimosaceae): Stem, roots, and seeds in the economy of the savanna areas of Nigeria. *Economic Botany*, 58(1), S34-S42. [https://doi.org/10.1663/0013-0001\(2004\)58\[s34:pamsra\]2.0.co;2](https://doi.org/10.1663/0013-0001(2004)58[s34:pamsra]2.0.co;2)
- Alshahrani, H., & Prakash, V. R. A. (2023). Development of highly flexible electromagnetic interference shielding composites for electronic applications using Cobalt/ Hevea brasiliensis seed husk carbon dots/ Bamboo microfibre-polyvinyl alcohol. *Industrial Crops and Products*, 191(PA), Article 115967. <https://doi.org/10.1016/j.indcrop.2022.115967>
- Azman, N. I. Z., Othman, M. K., Zaini, N. A. A., & Jusoh, M. A. (2022). Graphene-based materials for microstrip patch antenna. *Progress In Electromagnetics Research C*, 126, 207–216. <https://doi.org/10.2528/PIERC22090505>
- Babani, S., Hamidon, M. N., Ismail, A., & Jaafar, H. (2024a). Advancing microstrip patch antennas through *Prosopis africana* conductive ink-based thick films for enhanced bandwidth in radar applications. *Progress In Electromagnetics Research B*, 105, 17–29. <https://doi.org/10.2528/PIERB23122102>
- Babani, S., Nizar, M., Alyani, H., Haslina, I., Intan, J., & Hassan, H. (2024b). Development and characterization of screen - Printed *Prosopis Africana* Char thick film for electronic applications. *Journal of the Australian Ceramic Society*, 60(2), 643-652. <https://doi.org/10.1007/s41779-024-00999-8>
- Babani, S., Hamidon, M. N., Ismail, A., Jaafar, H., Bakar, A. A., & Lawal, I. (2023, September 12-13). *Impact of micrometer and nanometer-sized particles on the electrical properties of Prosopis africana biochar thick films*. [Paper presentation]. In 7th International Symposium on Advanced Materials and Nanotechnology (iSAMN2023), Serdang, Selangor.
- Babani, S., Hamidon, M. N., Ismail, A., Jaafar, H., Hassan, I. H., Shafee, F. N., Shitu, I. G., Yunusa, Z., Lamido, J., & Muhammad, S. (2025). Deployment of *Prosopis Africana* biomass material as a conductive thick film paste for electronic applications. In *Proceedings of the International Conference on Sustainability: Developments and Innovations* (pp. 125-132). Springer Nature Singapore. https://doi.org/10.1007/978-981-97-8712-8_16
- Babani, S., Khamis, N. H. H., Bala, B. D., & Ahmed Mohammed, T. A. (2015). A compact microstrip patch antenna for ADS-B operation. In *2014 IEEE Asia-Pacific Conference on Applied Electromagnetics (APACE)* (pp. 250-252). IEEE.. <https://doi.org/10.1109/APACE.2014.7043793>
- Bakar, A. A., Hamidon, M. N., Yaacob, M. H., Paiman, S., Jaafar, H., Jusoh, W. N. W., Shffee, F. N., & Hasan, I. H. (2023). An ohmic contact behavior of flexible thick film carbon-based electrode with TiO2 layer

at different operating temperature. *International Journal of Chemical and Biochemical Sciences*, 24(7), 246-252

- Bansal, R. (2008). Antenna theory; analysis and design. *Proceedings of the IEEE* 72(7), 989-990. <https://doi.org/10.1109/proc.1984.12959>
- Bishop, B., Abang, F. B. P., & Attah, S. (2021). Effect of Fermentation with rumen content on the feeding value of boiled iron tree (*Prosopis Africana*) seedcoat on haematology and serum biochemistry of broiler chickens. *Annual Research & Review in Biology*, 36, 70–77. <https://doi.org/10.9734/arrb/2021/v36i1230464>
- Chen, J., Li, J., Xiong, D., He, Y., Ji, Y., & Qin, Y. (2016). Preparation and tribological behavior of Ni-graphene composite coating under room temperature. *Applied Surface Science*, 361, 49–56. <https://doi.org/10.1016/j.apsusc.2015.11.094>
- Dakshayani, P., & Suryanarayana, V. (2022). Investigation of conformal CPW fed copper and multiwalled carbon nanotube microstrip antennas in X- band applications. *International Journal of Innovative Research and Practices*, 10(8), 6–11.
- Devi, K. S. C., Angadi, B., & Mahesh, H. M. (2017). Multiwalled carbon nanotube-based patch antenna for bandwidth enhancement. *Materials Science & Engineering B*, 224, 56–60. <https://doi.org/10.1016/j.mseb.2017.07.005>
- Garg, R., Bhartia, P., Bahl, I. J., & Ittipiboon, A. (2001). *Microstrip antenna design handbook*. Artech House.
- Guo, Y., Wei, X., Gao, S., Yue, W., Li, Y., & Shen, G. (2021). Recent advances in carbon material-based multifunctional sensors and their applications in electronic skin systems. *Advanced Functional Materials*, 31(40), Article 2104288. <https://doi.org/10.1002/adfm.202104288>
- Hasan, I. H., & Hamidon, M. N. (2017). Yttrium iron garnet thick film inclusion for enhanced microstrip patch antenna performance. In *2017 IEEE Regional Symposium on Micro and Nanoelectronics (RSM)* (pp. 131-134). IEEE. <https://doi.org/10.1109/RSM.2017.8069168>
- Hasan, I. H., Hamidon, M. N., Ismail, A., Ismail, I., Mekki, A. S., Mohd Kusaimi, M. A., Azhari, S., & Osman, R. (2018). YIG thick film as substrate overlay for bandwidth enhancement of microstrip patch antenna. *IEEE Access*, 6, 32601–32611. <https://doi.org/10.1109/ACCESS.2018.2842749>
- Huo, K. L., Yang, S. H., Zong, J. Y., Chu, J. J., Wang, Y. D., & Cao, M. S. (2023). Carbon-based EM functional materials and multi-band microwave devices: Current progress and perspectives. *Carbon*, 213, Article 118193. <https://doi.org/10.1016/j.carbon.2023.118193>
- Husain, Z., Shakeelur Rahman, A. R., Ansari, K. B., Pandit, A. B., Khan, M. S., Qyyum, M. A., & Lam, S. S. (2022). Nano-sized mesoporous biochar derived from biomass pyrolysis as electrochemical energy storage supercapacitor. *Materials Science for Energy Technologies*, 5, 99–109. <https://doi.org/10.1016/j.mset.2021.12.003>
- Khair, N., Islam, R., & Shahariar, H. (2019). Carbon-based electronic textiles: Materials, fabrication processes and applications. *Journal of Materials Science*, 54(14), 10079–10101. <https://doi.org/10.1007/s10853-019-03464-1>

- Kiffie, Z., Solomon, M., & Kassahun, S. K. (2023). Statistically optimized charcoal production from *Prosopis juliflora* for use as alternative fuel in cement factories. *Biomass Conversion and Biorefinery*, 13(3), 1539–1552. <https://doi.org/10.1007/s13399-020-01172-4>
- Kusaimi, M. A., Hamidon, M. N., & Azhari, S. (2018). Importance of annealing temperature on the electrical conductivity of screen printed graphite organic paste. *eProceedings Chemistry*, 3, 22-24.
- Leng, L., Xiong, Q., Yang, L., Li, H., Zhou, Y., Zhang, W., Jiang, S., Li, H., & Huang, H. (2021). An overview on engineering the surface area and porosity of biochar. *Science of the Total Environment*, 763, Article 144204. <https://doi.org/10.1016/j.scitotenv.2020.144204>
- Lu, G., Wang, J., Xie, Z., & Yeow, J. (2022). Carbon-based THz microstrip antenna design: A review. *IEEE Open Journal of Nanotechnology*, 3, 15–23. <https://doi.org/10.1109/OJNANO.2021.3135478>
- Lu, G., Wang, J., Xie, Z., & Yeow, J. T. W. (2021). Carbon-based THz microstrip antenna design: A review. *IEEE Open Journal of Nanotechnology*, 3, 15–23. <https://doi.org/10.1109/OJNANO.2021.3135478>
- Muhammad, S., Tiang, J. J., Wong, S. K., Iqbal, A., Smida, A., & Azizi, M. K. (2021). A compact dual-port multi-band rectifier circuit for RF energy harvesting. *Computer Materials & Continua*, 68(1), 167-184. <https://doi.org/10.32604/cmc.2021.016133>
- Musa, U., Babani, S., Babale, S. A., Ali, A. S., Yunusa, Z., & Lawan, S. H. (2023). Bandwidth enhancement of millimeter-wave microstrip patch antenna array for 5G mobile communication networks. *Bulletin of Electrical Engineering and Informatics*, 12(4), 2203–2211. <https://doi.org/10.11591/eei.v12i4.4680>
- Nnamani, P. O., Shinde, J. A., Jadhav, R. N., Sanandam, M. R., & Lokhande, C. D. (2020). Fundamental properties of *Prosopis Africana* peel powders (PAPPs) as drug delivery excipient. *African Journal of Pharmaceutical Research & Development*, 12(1), 119–133.
- Quaranta, S., Giorcelli, M., & Savi, P. (2019). Graphene and MWCNT printed films: Preparation and RF electrical properties study. *Journal of Nanomaterials*, 2019(1), Article 4658215. <https://doi.org/10.1155/2019/4658215>
- Ram, P., Yadav, A., Suman, M. K., & Kumar, A. (2021). Graphene based circular shaped micro strip patch antenna array for 2.45 GHz ISM band application. *Wireless Personal Communications*, 116(3), 1613–1620. <https://doi.org/10.1007/s11277-020-07751-y>
- Rao, T. R., & Sharma, A. (1998). Pyrolysis rates of biomass materials. *Energy*, 23(11), 973-978.
- Rizwan, M., Member, S., Waqas, M., Khan, A., Member, S., Syd, L., Virkki, J., & Ukkonen, L. (2017). Flexible and stretchable brush-painted wearable antenna on a three-dimensional (3-D) printed substrate. *IEEE Antennas and Wireless Propagation Letters*, 16, 3108-3112. <https://doi.org/10.1109/LAWP.2017.2763743>
- Sa'don, S. N. H., Jamaluddin, M. H., Kamarudin, M. R., Ahmad, F., & Dahlan, S. H. (2019). A 5G graphene antenna produced by screen printing method. *Indonesian Journal of Electrical Engineering and Computer Science*, 15(2), 950–1055. <https://doi.org/10.11591/ijeecs.v15.i2.pp950-955>
- Shafee, F. N., Hamidon, M. N., Wahid, M. H., Shaari, A. H., Ertugrul, M., Abdullah, N. H., Kusaimi, M. A. M., Mustafa, M. S., & Ibrahim, I. R. (2020). Effect of nanometric and micronic particles size on physical and electrical properties of graphite thick film. *International Journal of Nanotechnology*, 17(11–12), 825–839. <https://doi.org/10.1504/IJNT.2020.112385>

- Shitu, I. G., Katibi, K. K., Muhammad, A., Chiromawa, I. M., Tafida, R. A., Amusa, A. A., & Babani, S. (2023). Effects of irradiation time on the structural, elastic, and optical properties of hexagonal (wurtzite) zinc oxide nanoparticle synthesised via microwave-assisted hydrothermal route. *Optical and Quantum Electronics*, 56(2), 266. <https://doi.org/10.1007/s11082-023-05867-6>
- Shitu, I. G., Katibi, K. K., Tafida, R. A., Iya, S. G. D., Alotaibi, K. M., Babani, S., Amusa, A. A., Elbidi, M., Katibi, M. T., & Mallik, S. (2024). Synthesis and characterization of magnetic biochar nanocomposite from oil palm fronds for efficient copper (II) ion removal from leachate. *Clean Technologies and Environmental Policy*. <https://doi.org/10.1007/s10098-024-03041-4>
- Song, R., Huang, G., Liu, C., Zhang, N., Zhang, J., Liu, C., Wu, Z. P., & He, D. (2019). High-conductive graphene film based antenna array for 5G mobile communications. *International Journal of RF and Microwave Computer-Aided Engineering*, 29(6), Article e21692.
- Su, Y., Guo, Z., Huang, W., Liu, Z., Gong, T., He, Y., & Yu, B. (2016). Ultra-sensitive graphene photodetector with plasmonic structure. *Applied Physics Letters*, 109(17), Article 173107. <https://doi.org/10.1063/1.4966597>
- Sumaila, J. L., Sani, D., Aibu, S., Hamidon, M. N., Yunusa, Z., Magaji, N., Abubakar, A., Shafiee, F. N., & Babani, S. (2023a). Morphology and electrical properties of pristine and composite rice husk ash nano / micro particles thick films for gas sensing applications. In *2023 IEEE Regional Symposium on Micro and Nanoelectronics (RSM)* (pp. 90-93). IEEE. <https://doi.org/10.1109/RSM59033.2023.10327321>
- Sumaila, J. L., Sani, D., Magaji, N., & Yunusa, Z. (2023b). Rice husk ash (RHA) nano particles as new materials for hydrogen gas sensor. In *Proceeding of 7th International Symposium on Advanced Materials and Nanotechnology* (pp. 136–139). Institut of Nanoscience and Nanotechnology Universiti Putra Malaysia.
- Tovar-Lopez, F. J. (2023). Recent progress in micro- and nanotechnology-enabled sensors for biomedical and environmental challenges. *Sensors*, 23(12), Article 5406. <https://doi.org/10.3390/s23125406>
- Yan, B., Zheng, J., Feng, L., Du, C., Jian, S., Yang, W., Wu, Y. A., Jiang, S., He, S., & Chen, W. (2022). Wood-derived biochar as thick electrodes for high-rate performance supercapacitors. *Biochar*, 4(1), Article 50. <https://doi.org/10.1007/s42773-022-00176-9>
- Yunusa, Z., & Musa, U. (2023). Rheological properties of *Prosopis Africana* Char paste thick film for antenna applications. In *2023 IEEE International Conference on Sensors and Nanotechnology (SENNANO)* (pp. 37-40). IEEE. <https://doi.org/10.1109/SENNANO57767.2023.10352532>
- Yunusa, Z., & Shehu, A. A. (2022). Comparative study of single-slot and multi-slot graphene-based microstrip patch antenna for X-band application. *NanoEra*, 2(1), 1-4.
- Yusuf, N. D., Ogah, D. M., Hassan, D. I., Musa, M. M., & Doma, U. D. (2008). Effect of decorticated fermented prosopis seed meal (*Prosopis Africana*) on growth performance of broiler chicken. *International Journal of Poultry Science*, 7(11), 1054–1057. <https://doi.org/10.3923/ijps.2008.1054.1057>